Supporting Information for

Cationic donor–π–acceptor AIEgen enabling dual-mode reactive oxygen species generation for antibacterial photodynamic therapy

Hongyu Dai[a], Zeyao Yu[b], Yuanpeng Song[a], Riliga Wu[a], Chengcheng Zhou[b], Yang Liu,*[c] Weijiang Guan*[,a] and Chao Lu*[,a,d]

[a]*State Key Laboratory of Chemical Resource Engineering, Beijing University of Chemical Technology, Beijing 100029, China.*

[b]*School of Chemistry and Chemical Engineering, Yangzhou University, Yangzhou 225002, China.*

[c]*Center of Basic Medical Research, Institute of Medical Innovation and Research, Peking University Third Hospital, Beijing 100191, China.*

[d]*Pingyuan Laboratory, College of Chemistry, Zhengzhou University, Zhengzhou 450001, China.*

Experimental section

Chemicals and Materials. 1-(4-Bromophenyl)-1,2,2-triphenylethylene (TPE-Br), tetrakis(triphenylphosphine)palladium ($Pd(PPh_3)_4$), 5-formyl-2-thiopheneboronic acid, peptone from casein, yeast extract, chlorin e6 (Ce6), 2',7'-dichlorodihydrofluorescein diacetate (DCFH-DA), and 2,2'-(anthracene-9,10-diylbis(methylene))dimalonic acid (ABDA) were sourced from Energy Chemical Co., Ltd (Shanghai, China). Dihydrorhodamine 123 (DHR123), rose bengal (Rb) and hydroxyphenyl fluorescein (HPF) were procured from Shanghai Macklin Biochemical Co., Ltd (Shanghai, China). 1,4-Dimethylpyridinium iodide was obtained from Heowns Biochem Technologies (Tianjin, China). Cesium carbonate (Cs_2CO_3) was sourced from J&K Scientific Ltd. (Beijing, China). Sodium chloride (NaCl) and anhydrous sodium sulfate (Na_2SO_4) were purchased from Aladdin Biochemical Technology Co., Ltd. (Shanghai, China). Phosphate buffer saline (PBS, pH = 7.4) was purchased from wisent corporation (Nanjing, China). Ethanol (EtOH), piperidine, n-hexane, ethyl acetate (EA), tetrahydrofuran (THF), methanol (MeOH), acetonitrile (ACN), dimethyl sulfoxide (DMSO), and dichloromethane (DCM) were procured from Beijing Chemical Reagent Company (Beijing, China). *S. aureus* (ATCC6538) was obtained from the Beijing Microbiological Culture Collection Center (Beijing, China).

Instrumentation and Characterization. Nuclear magnetic resonance spectra for proton (^{1}H NMR) and carbon-13 (^{13}C NMR) were obtained by utilizing a Bruker AV 600 spectrometer (Bruker, Germany). Mass spectrometry (MS) was performed using a Quattro micro-triple quadrupole mass spectrometer (Waters, USA). Transmission electron microscopy (TEM) image was obtained by an HT7700 transmission electron microscope (Hitachi, Japan). Dynamic light scattering (DLS) tests were conducted utilizing a Zetasizer Nano ZS (Malvern, UK). Fluorescence spectra were acquired using an F-7000 fluorescence spectrophotometer (Hitachi, Japan) with a slit width of 5.0 nm and a scanning rate of 2400 nm/min. Ultraviolet–visible (UV–vis) absorption spectra were recorded employing a U-3900H spectrometer (Hitachi, Japan). Confocal images were captured employing a LSM 880NLO (Carl Zeiss, Germany). Scanning electron microscopy (SEM) images were obtained by Gemini SEM 300 (Carl Zeiss, Germany). A water-jacketed constant temperature incubator (GSP-9050MBE; BoXun, China) was employed to cultivate *S. aureus*. A white light source was purchased from Zixing Chuanshiyuan General Trading Company (XML-T6, Chenzhou, China).

Synthesis of Intermediate 2. TPE-Br (500 mg, 1.12 mmol), 5-formyl-2-thiopheneboronic acid (209 mg, 1.34 mmol), Cs_2CO_3 (730 mg, 2.24 mmol), and $Pd(PPh_3)_4$ (100 mg, 0.086 mmol) were added in a 250 mL of three neck flask. 40 mL of THF, 40 mL of MeOH, and 10 mL of H_2O were added under N_2 atmosphere. The mixture was stirred and refluxed at 120 °C for 24 h. After cooling, the compound extracted with EA. The collected organic layer was dried with Na_2SO_4 and evaporated to dryness. The residue was subjected to column chromatography (n-hexane:EA = 6:1). The obtained product was a light-yellow powder with 56.2% yield. ^{1}H NMR (600 MHz, DMSO-d_6, δ): 9.89 (s, 1H), 8.00-8.01 (d, 1H), 7.67-7.68 (d, 1H), 7.58-7.60 (d, 2H), 7.10-7.17 (m, 9H), 6.97-7.06 (m, 8H). ^{13}C NMR (151 MHz, DMSO-d_6, δ): 184.45, 152.68, 145.06, 143.44, 143.41, 143.26, 142.26, 141.88, 140.18, 139.72, 132.10, 131.98, 131.19, 131.14, 131.09, 130.90, 129.13, 128.49, 128.42, 128.29, 127.34, 127.21, 127.16, 126.07, 125.66. HRMS (ESI) m/z: calculated for $C_{31}H_{23}OS^+$ $[M+H]^+$ 443.1391; found 443.1374.

Synthesis of TTMPy. 1,4-Dimethylpyridinium iodide (70 mg, 0.3 mmol) dissolved in 10 mL of EtOH. Then, a few drops of piperidine were added, and the mixture stirred at room temperature for 12 min. Afterward, a 10 mL of EtOH solution of compound 2 (110 mg, 0.25 mmol) was added to the mixture. The mixture was refluxed overnight. After cooling, the organic solvent was removed. The residue was subjected to column chromatography (DCM:MeOH = 20:1). The obtained product was dark red powder with 42.6% yield. ^{1}H NMR (600 MHz, DMSO-d_6, δ): 8.82-8.84 (d, 2H), 8.17-8.23 (t, 3H), 7.57-7.58 (d, 1H), 7.50-7.52 (d, 3H), 7.12-7.18 (m, 10H), 6.97-7.02 (m, 8H), 4.23 (s, 3H). ^{13}C NMR (151 MHz, DMSO-d_6, δ): 152.56, 146.98, 145.36, 144.14, 143.49, 143.34, 141.70, 140.29, 140.07, 134.07, 133.83, 132.08, 132.00, 131.38, 131.20, 131.15, 131.09, 129.13, 128.48, 128.42, 128.30, 127.30, 127.20, 127.14, 125.80, 125.45, 123.55, 122.28, 47.26. HRMS (ESI) m/z: calculated for $C_{38}H_{30}NS^+$ $[M-I]^+$ 532.2094; found 532.2098.

Preparation of TTMPy Nanoparticles. TTMPy was first dissolved in DMSO to form a 1 mM stock solution. Then, 10 μL of this solution was injected into 990 μL of deionized water under vigorous stirring, resulting in the formation of TTMPy nanoparticles due to nanoprecipitation. The suspension was further stirred for 30 min and then filtered through a 0.22 μm membrane to remove large aggregates. The obtained nanoparticles were stored in light-protected vials at 4 °C.

Computational Methods. Geometry optimizations were performed using the Beijing Density Functional (BDF) program, and harmonic frequency calculations were carried out at the same level of theory to confirm that all optimized structures had no imaginary frequencies. The highest occupied molecular orbital (HOMO) and lowest unoccupied molecular orbital (LUMO) isosurfaces were rendered using Visual Molecular Dynamics (VMD) based on files generated by Multiwfn 3.8 (dev).

ROS Detection. The ROS generation was measured by using DCFH-DA as indicator. The probe was first activated through the general method. 0.25 mL of 1 mM DCFH-DA in ethanol was added into 1 mL NaOH (10 mM), and the solution was stirred for half an hour at room temperature. The hydrolysis product (DCFH) was neutralized with 5 mL PBS and stored on ice for later use. For ROS detection, 40 μM DCFH was mixed with PS (10 μM) in H_2O/DMSO (99:1, v/v) and exposed to white light (20 mW/cm^2). The probe was monitored by recording the emission increment at 525 nm with the excitation of 488 nm.

$^1O_2$ Detection. The $^1O_2$ generation was measured by using ABDA as indicator. ABDA (50 μM) was mixed with PS (10 μM) in H_2O/DMSO (99:1, v/v) and exposed to white light (20 mW/cm^2). The probe was monitored by recording the absorbance decrease at 378 nm.

$O_2^{\bullet-}$ Detection. The $O_2^{\bullet-}$ generation was measured by using DHR123 as indicator. DHR123 (10 μM) was mixed with PS (10 μM) in H_2O/DMSO (99:1, v/v) and exposed to white light (20 mW/cm^2). The probe was monitored by recording the emission increment at 530 nm with the excitation of 488 nm.

$^\bullet OH$ Detection. The $^\bullet OH$ generation was measured by using HPF as indicator. HPF (10 μM) was mixed with PS (10 μM) in H_2O/DMSO (99:1, v/v) and exposed to white light (20 mW/cm^2). The probe was monitored by recording the emission increment at 520 nm with the excitation of 490 nm.

Quantum Yield of $^1O_2$. The $^1O_2$ quantum yield (Φ) of TTMPy was determined using Rb as a reference according to the following equation:

$$\Phi_{TTMPy} = \frac{\Phi_{Rb} \times K_{TTMPy} \times A_{Rb}}{K_{Rb} \times A_{TTMPy}}$$

where K is the ABDA decomposition rate constant and A is the integrated absorbance in the 400–800 nm range. The Φ value of Rb was taken as 0.75 in water.

Retention Ability of $^1O_2$. The retention ability for $^1O_2$ was evaluated using ABDA as a probe. Three PSs were first irradiated with white light for 60 s. Subsequently, the white light irradiation was turned off, and the absorbance of ABDA was measured at 10 s and 20 s after cessation of irradiation.

Preparation of *S. aureus* Suspension. A single colony of *S. aureus* was inoculated into 10 mL of Luria–Bertani (LB) medium (containing 10 g/L peptone from casein, 5 g/L yeast extract, and 10 g/L NaCl) and cultured at 37 °C with shaking at 180 rpm for 8–10 h. *S. aureus* was collected by centrifuging for 2 min at 7000 rpm to remove the supernatant, washed twice with PBS, and resuspended in PBS. The bacterial concentration was adjusted to OD_{600nm} = 1.0, corresponding to approximately 10^8 colony-forming units per milliliter (CFU/mL) of *S. aureus*.

Evaluation of Antibacterial Activity. The antibacterial activity of compound TTMPy against *S. aureus* at different concentrations was evaluated using the standard plate counting method. Both dark and light conditions were assessed. For the dark condition, the *S. aureus* suspension in PBS was incubated with various concentrations of TTMPy at 37 °C in the dark for 30 min. For the light condition, the suspension was exposed to white light (40 mW/cm^2) for 30 min at 37 °C. After treatment, the suspensions were diluted 10^5-fold with PBS, and 100 µL of each diluted sample was evenly spread on LB agar plates. Each concentration group was tested in triplicate. The plates were incubated at 37 °C for 14–16 h, and the number of colonies was counted. The bactericidal survival rate of TTMPy was calculated using the following equation:

$$Survival\ rate\ (\%) = \frac{B}{A} \times 100\%$$

where A is the number of CFU in the control group, and B is the CFU count in the experimental group.

Morphological Analysis of *S. aureus*. The morphology of *S. aureus* before and after treatment with TTMPy was examined by SEM. Following the antibacterial activity assessment, *S. aureus* was treated with 5 µM TTMPy. The cells were collected by centrifugation (7000 rpm, 5 min) without dilution, resuspended in 100 µL of sterile water, and 5 µL of the suspension was dropped onto a clean silicon slice. After airdrying in a biosafety cabinet, the silicon slice was immersed in 0.1% glutaraldehyde in PBS and fixed overnight. The sample was washed with sterile water three times and dehydrated with gradient ethanol (60%, 70%, 90%, and 100%). After drying under vacuum, the specimen was sputter-coated with gold for SEM observation.

Confocal Imaging. A suspension of *S. aureus* in PBS (100 μL, OD_{600nm} = 1.0) was incubated with TTMPy (5 μM) in 400 μL of PBS for 0, 10, 20, and 30 min. After centrifugation (7000 rpm, 2 min) to remove the supernatant, the remaining *S. aureus* was resuspended in 50 μL of PBS. 5 μL of the as-prepared *S. aureus* suspension was dripped on a glass slide and covered with a coverslip. Then the imaging was performed on a confocal microscope with the excitation wavelength of 430 nm and the emission wavelength of 500–700 nm.

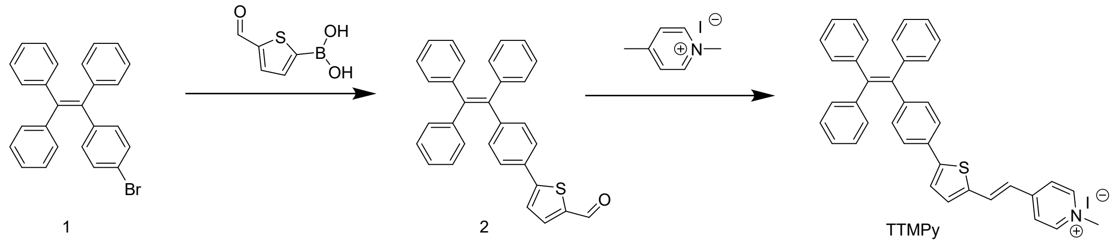

Fig. S1. Synthesis route of TTMPy.

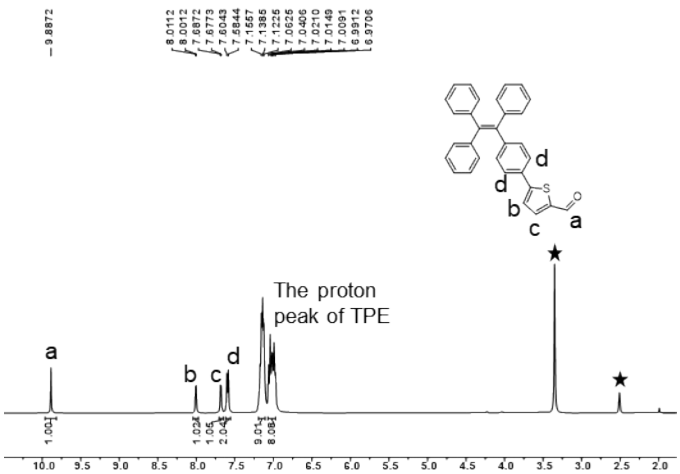

Fig. S2. ^{1}H NMR spectrum of intermediate 2 in DMSO-d_6. Asterisks indicate solvent peaks, namely water and DMSO.

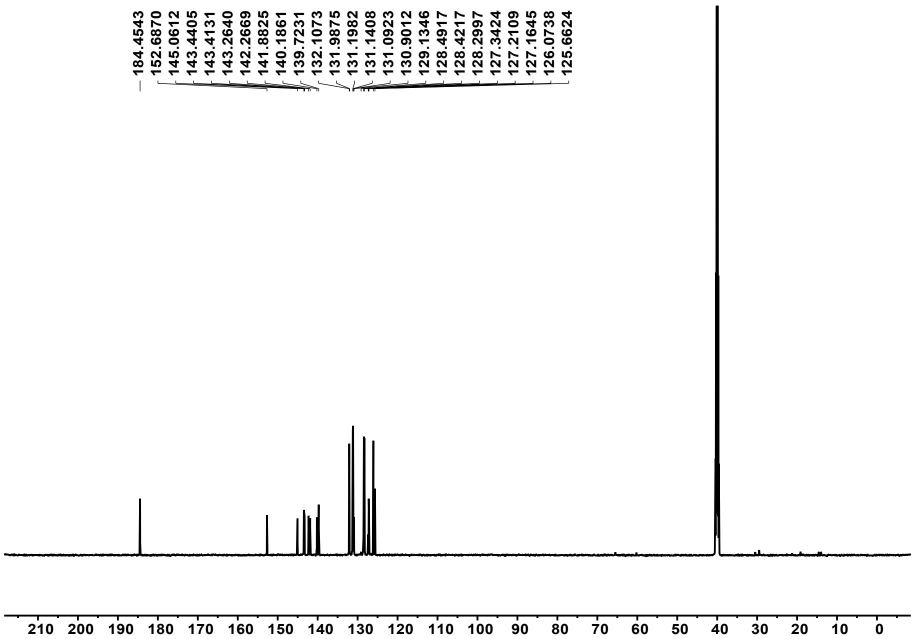

Fig. S3. ^{13}C NMR spectrum of intermediate 2 in DMSO-d_6.

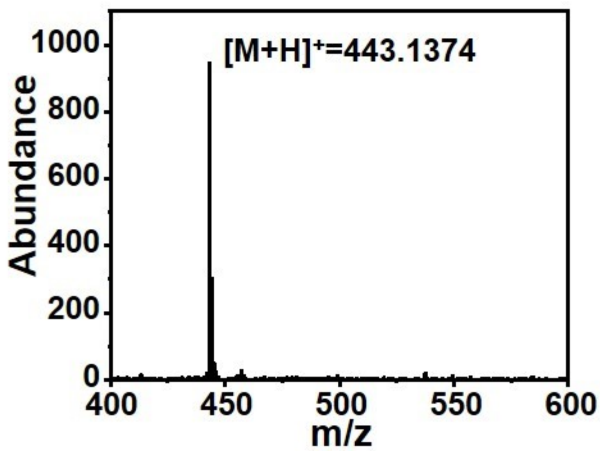

Fig. S4. Positive-ion mode MS spectrum of intermediate 2.

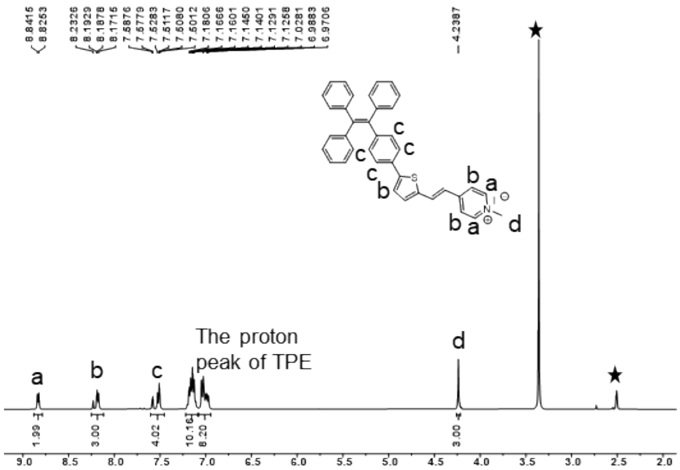

Fig. S5. ^{1}H NMR spectrum of TTMPy in DMSO-d_6. Asterisks indicate solvent peaks, namely water and DMSO.

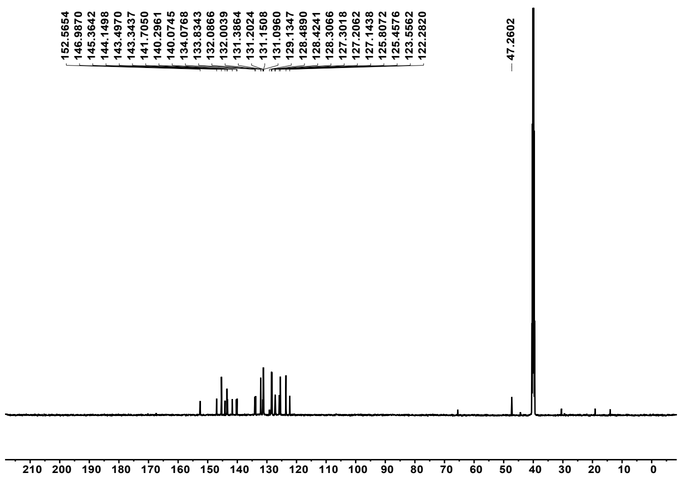

Fig. S6. ^{13}C NMR spectrum of TTMPy in DMSO-d_6.

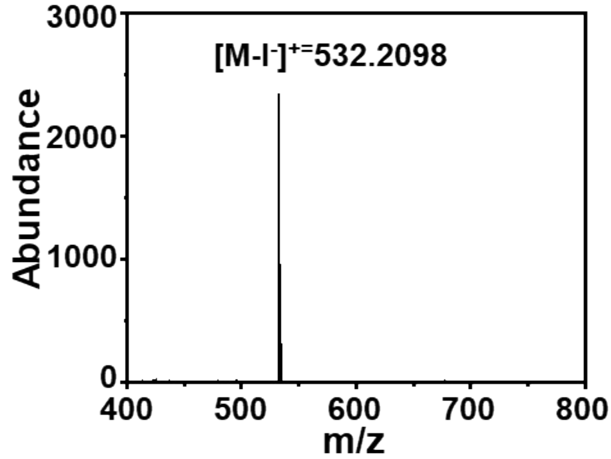

Fig. S7. Positive-ion mode MS spectrum of TTMPy.

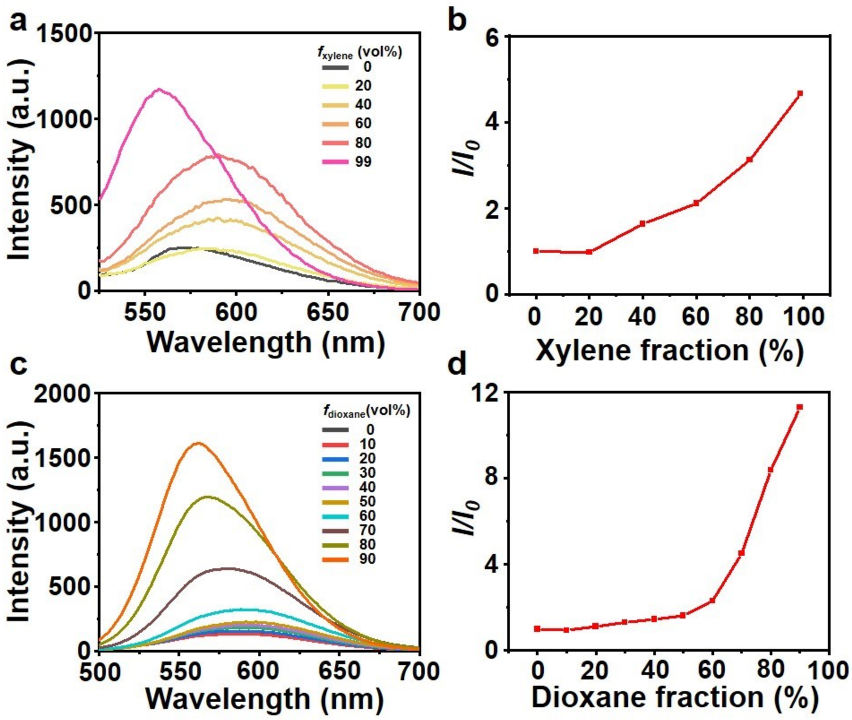

Fig. S8. (a) Fluorescence spectra of TTMPy in MeOH/xylene mixtures with different xylene fractions, and (b) the corresponding plot of relative fluorescence intensity (I/I_0) versus xylene fraction; (c) fluorescence spectra of TTMPy in MeOH/dioxane mixtures with different dioxane fractions, and (d) the corresponding plot of relative fluorescence intensity (I/I_0) versus dioxane fraction.

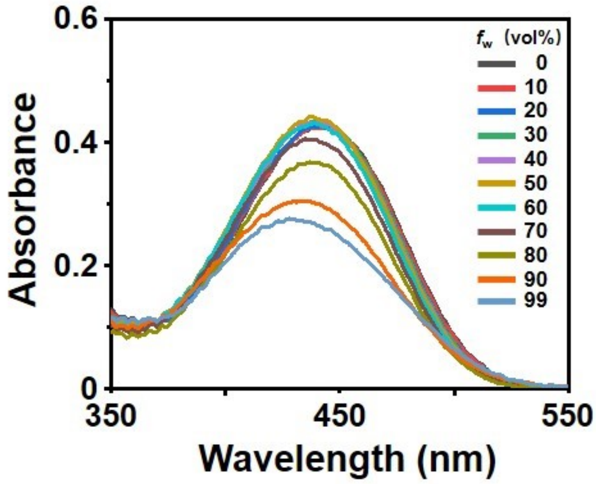

Fig. S9. Absorption spectra of 10 μM TTMPy in H_2O/DMSO mixtures with different water fractions.

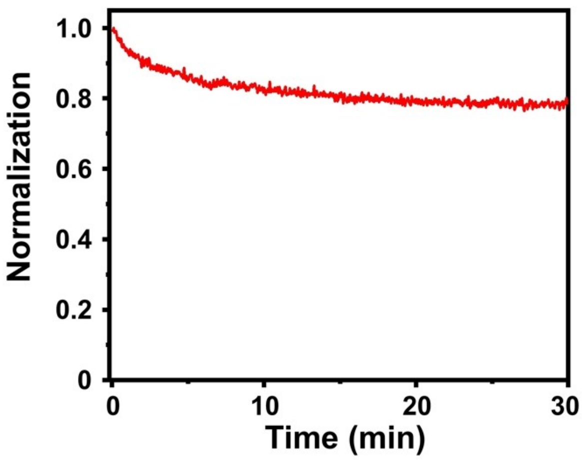

Fig. S10. Photostability of TTMPy nanoparticles (10 μM) in H_2O/DMSO (99:1, v/v) under 445 nm irradiation.

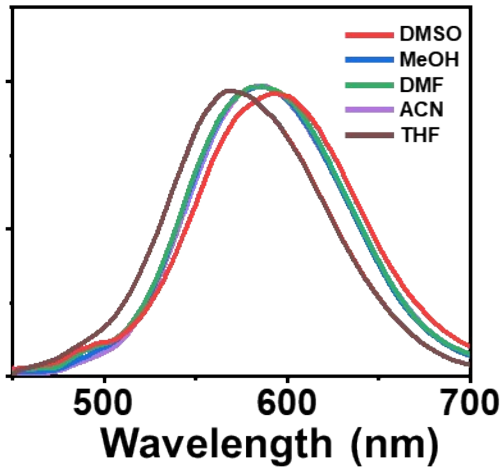

Fig. S11. Normalized solvent-dependent emission spectra of 10 μM TTMPy in various solvents.

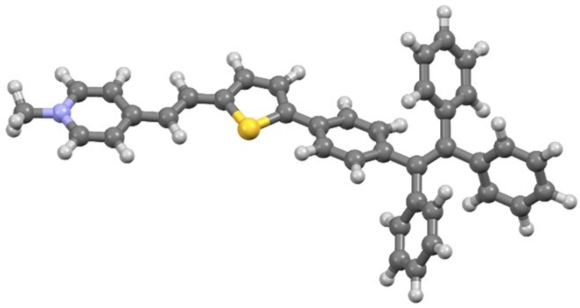

Fig. S12. Optimized molecular structure of TTMPy.

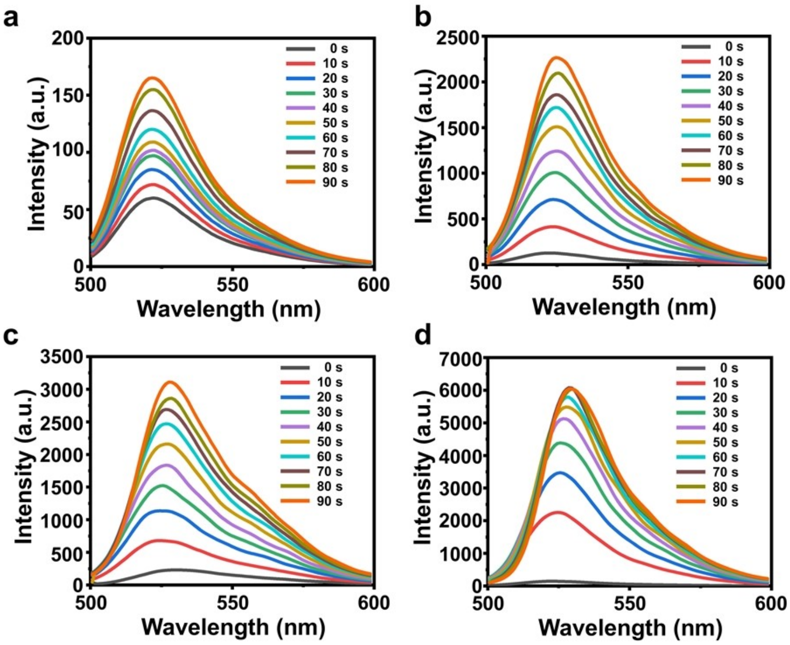

Fig. S13. Fluorescence emission spectra of DCFH in the absence (a) and the presence of (b) Ce6, (c) Rb, and (d) TTMPy. Concentration (40 μM for DCFH, 10 μM for photosensitizers), white light (20 mW/cm^2), λ_{ex} = 488 nm.

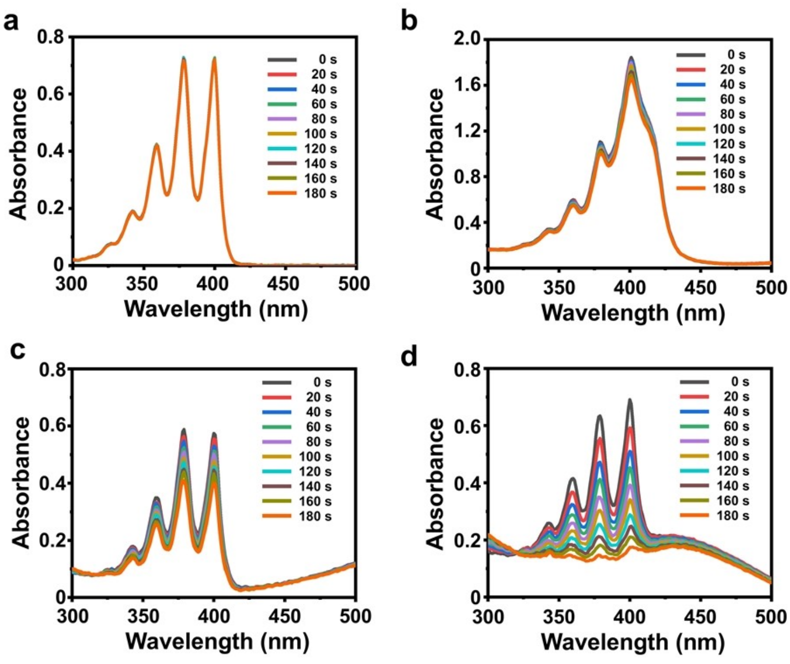

Fig. S14. Absorption spectra of ABDA in the absence (a) and the presence of (b) Ce6, (c) Rb, and (d) TTMPy. Concentration (50 μM for ABDA, 10 μM for photosensitizers), white light (20 mW/cm^2).

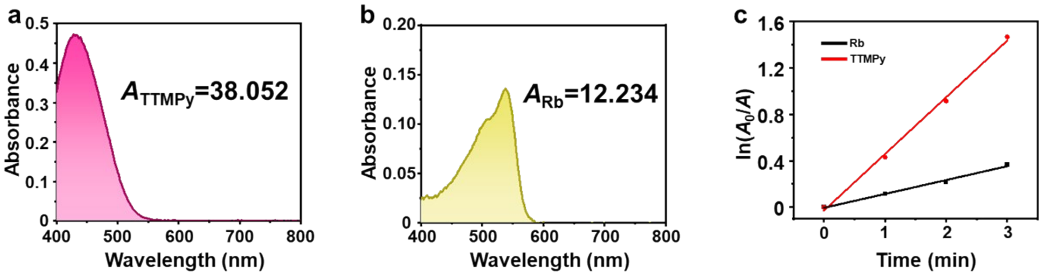

	Intercept		Slope		Statistics	$^1O_2$ Quantum yield
	Value	Standard Error	value	Standard Error	Adj. R-Square	
TTMPy	-0.02981	0.03637	0.4889	0.01944	0.99527	98.4%
Rose Bengal	-0.00545	0.01336	0.1197	0.00714	0.9894	75%

Fig. S15. Absorption spectra of (a) TTMPy and (b) Rb. (c) Decomposition rate of ABDA in the presence of TTMPy and Rb under white-light irradiation (20 mW/cm^2). The concentrations were 50 µM for ABDA and 10 µM for the PS.

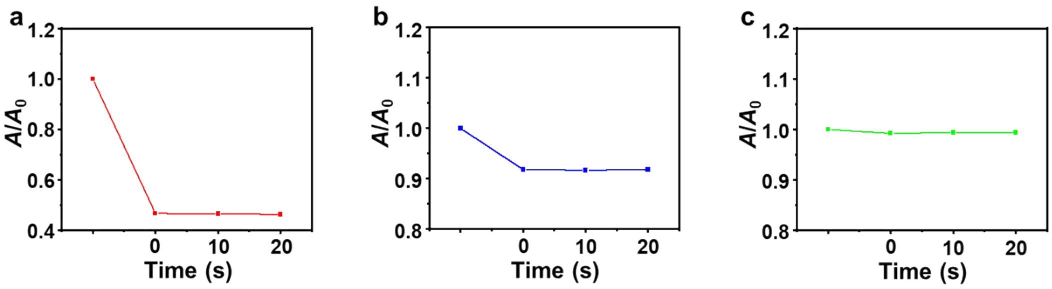

Fig. S16. Absorption changes of ABDA at 378 nm in the presence of (a) TTMPy, (b) Rb, and (c) Ce6 after 60 s of white-light irradiation (20 mW/cm^2). The concentrations were 50 µM for ABDA and 10 µM for the PS.

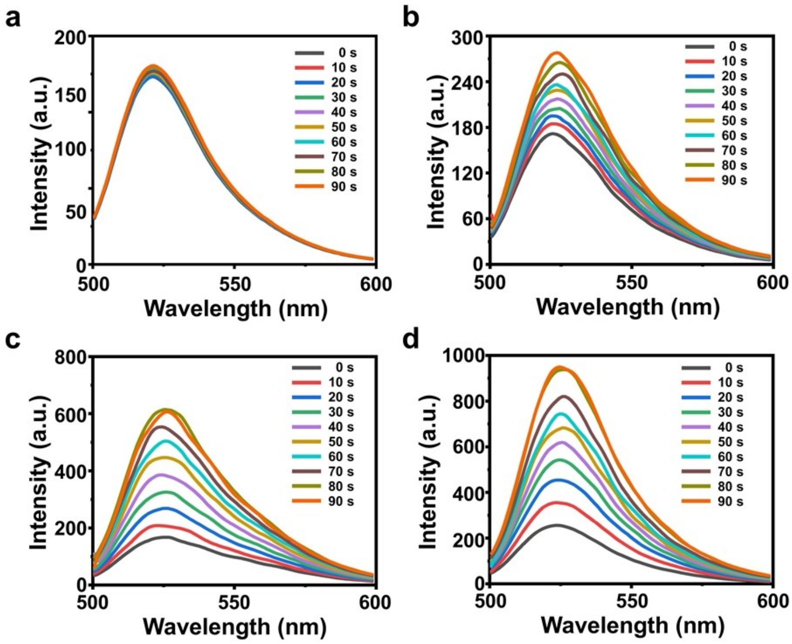

Fig. S17. Fluorescence emission spectra of DHR123 in the absence (a) and the presence of (b) Ce6, (c) Rb, and (d) TTMPy under white-light irradiation (20 mW/cm^2). The concentrations were 10 μM for DHR123 and 10 μM for the PS (λ_{ex} = 488 nm).

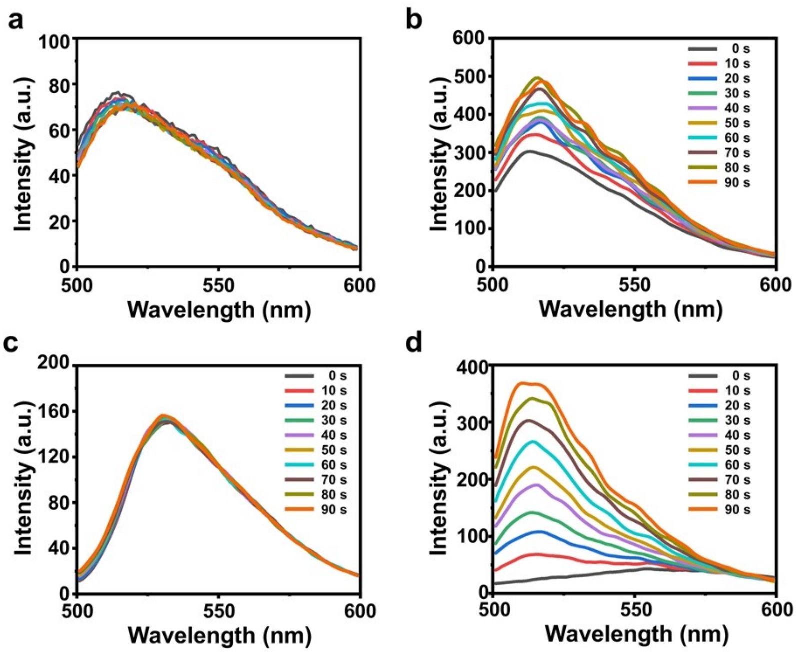

Fig. S18. Fluorescence emission spectra of HPF in the absence (a) and the presence of (b) Ce6, (c) Rb, and (d) TTMPy under white-light irradiation (20 mW/cm^2). The concentrations were 10 μM for HPF and the PS (λ_{ex} = 490 nm).

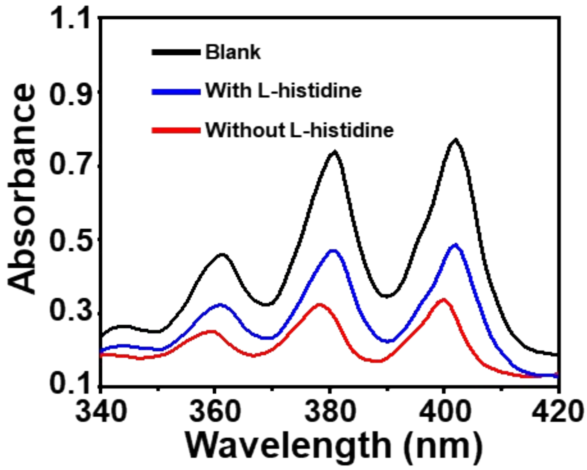

Fig. S19. Absorption spectra of ABDA as a $^1O_2$ probe with and without the addition of a $^1O_2$ scavenger (L-histidine) after 60 s of white-light irradiation (20 mW/cm^2).

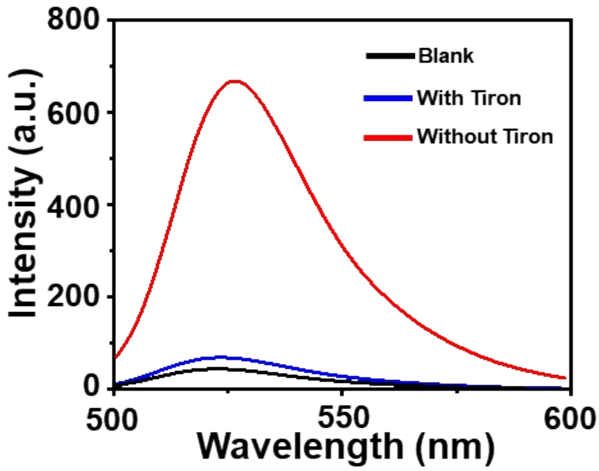

Fig. S20. Fluorescence spectra of DHR123 as a $O_2^{\bullet-}$ probe with and without the addition of a $O_2^{\bullet-}$ scavenger (Tiron) after 60 s of white-light irradiation (20 mW/cm^2).

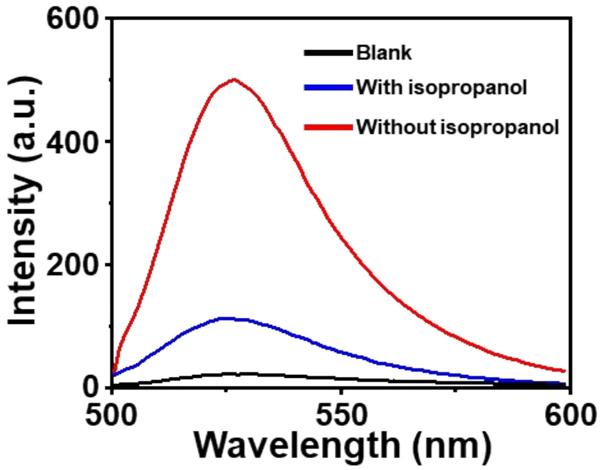

Fig. S21. Fluorescence spectra of HPF as a •OH probe with and without the addition of a •OH scavenger (isopropanol) after 60 s of white-light irradiation (20 mW/cm^2).

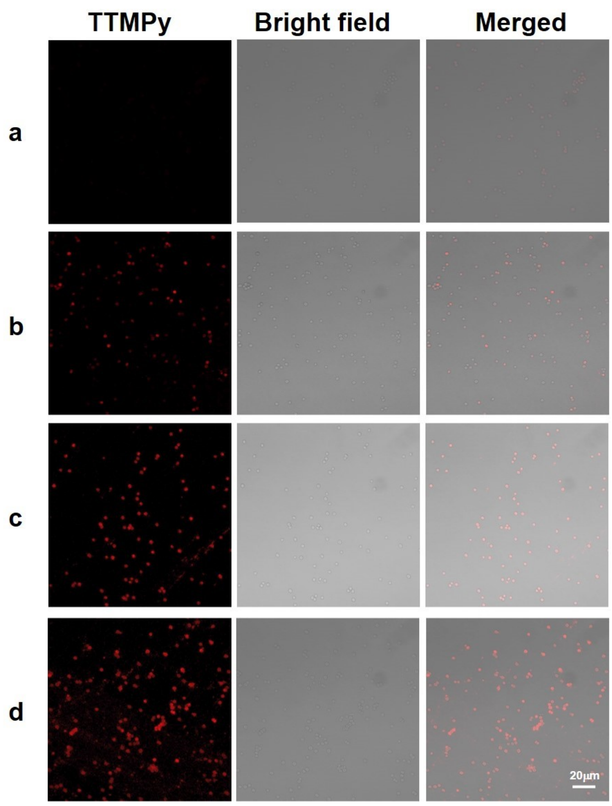

Fig. S22. Confocal laser scanning microscopy images of *S. aureus* after incubation for (a) 0 min, (b) 10 min, (c) 20 min and (d) 30 min, TTMPy channel (left), bright-field channel (middle), and merged images (right) are shown. Scale bar: 20 μm.

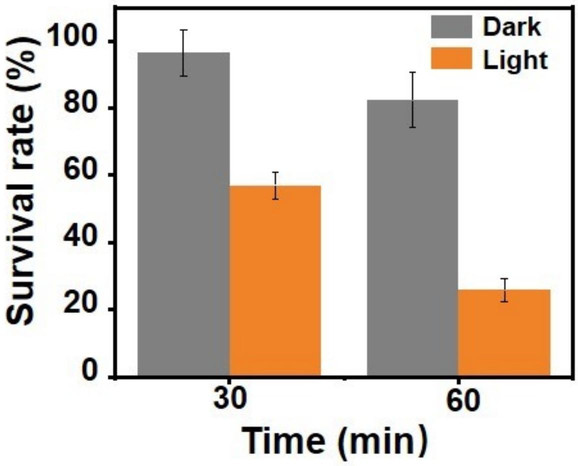

Fig. S23. Survival rate as a function of irradiation time at a TTMPy concentration of 1 μM under white-light irradiation (20 mW/cm^2).

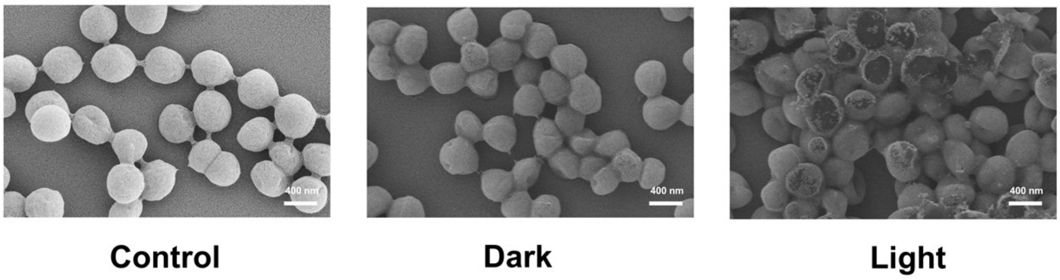

Fig. S24. SEM images of *S. aureus* after different treatments: control, TTMPy in the dark, and TTMPy with white-light irradiation. Scale bars: 400 nm.